Journal of Materials Chemistry C

PAPER

View Article Online
View Journal | View Issue

Cite this: J. Mater. Chem. C, 2015, 3, 5903

New AIEgens containing dibenzothiophene-*S*,*S*-dioxide and tetraphenylethene moieties: similar structures but very different hole/electron transport properties†

Xuejun Zhan,‡[a] Zhongbin Wu,‡[b] Yuxuan Lin,[a] Sheng Tang,[a] Jie Yang,[a] Jie Hu,[a] Qian Peng,[c] Dongge Ma,*[b] Qianqian Li[a] and Zhen Li*[a]

Received 13th April 2015,
Accepted 30th April 2015

DOI: 10.1039/c5tc01028d

www.rsc.org/MaterialsC

Three AIEgens were designed and constructed using tetraphenylethene and dibenzothiophene-*S*,*S*-dioxide, which show good thermal stability as verified by thermogravimetric and differential scanning calorimetry analyses. Single-carrier devices indicate that the control of the transport properties of these AIEgens can be realized by conveniently modifying the linkage mode of their two construction blocks. The obtained experimental results might open up a new option for the design of efficient blue AIEgens. Furthermore, when they are utilized as sky-blue emitting layers in OLEDs, the devices exhibit the highest efficiencies with the maximum external quantum efficiency of 3.62%, current efficiency of 8.66 cd A^{-1} and power efficiency of 5.28 lm W^{-1}.

Introduction

Nowadays, research on aggregation-induced emissions (AIE), which was pioneered by Ben Zhong Tang, is a very hot topic.[1] Many AIEgens have been successfully prepared and applied in different fields, including cell imaging, chemo/bio-sensors, light emitting diodes (LED), and field-effect transistors, with very promising performances.[2–8] Especially, some AIE-based LED devices demonstrated a very high external quantum efficiency of 8%, which approaches the theoretical limitation of OLEDs based on fluorescent luminogens;[9] moreover, some AIE-based field effect transistors exhibited good performances.[8] In general, to achieve a high efficiency of LEDs, the active materials used should simultaneously possess high hole and electron mobility.[10] Actually, because of the great efforts of scientists, some good strategies have been proposed for the design of new fluorophores and host materials for phosphorescent luminogens with good and balanced hole and electron mobility.[11] However, research on the transport properties of AIEgens is very scarce, and there are no reports concerning the design of AIEgens with balanced hole and electron mobility, regardless of the fact that many AIEgens have been synthesized and applied to LEDs, which have different emissions ranging from deep blue to red.[12–14]

As shown in Chart S1 (ESI†), for the construction of bipolar transport hosts with balanced high hole and electron mobility, p-type groups should be incorporated with an n-type group through different approaches, which have greatly suppressed intramolecular charge transfer. In other words, there should be some interactions between the p- and n-type moieties, but they should be very weak. This, in some sense, is similar to our design idea of controlling intramolecular conjugation for the design of blue or deep blue AIEgens,[15–17] in which the conjugation effect between the aromatic rings could be suppressed by utilizing different linkage modes or increasing the twisting degree of the molecules in the presence of additional groups. Then, how about these strategies being applied to the design of AIEgens with balanced high hole and electron mobility?

Dibenzothiophene-*S*,*S*-dioxide is a good electron withdrawing unit, which has been incorporated into polymers and small molecules in order to improve their electron transportation ability.[18–22] Moreover, it has an electron mobility of 10^{-4} cm^2 V^{-1} S^{-1} (close to the hole mobility of TPE unit), which may help the adjustment effect to occur.[17] Thus, in this study, prompted by the above points, three AIEgens, **DBTO-*p*TPE**, **DBTO-MeTPE** and **DBTO-*m*TPE** (Chart 1), were constructed using tetraphenylethene and dibenzothiophene-*S*,*S*-dioxide in which the TPE and DBTO moieties were linked together through different approaches. Regardless of the fact that they have similar structures,

[a] Department of Chemistry, Hubei Key Lab on Organic and Polymeric Opto-Electronic Materials, Wuhan University, Wuhan, 430072, China. E-mail: lizhen@whu.edu.cn, lichemlab@163.com; Fax: +86-27-68756757; Tel: +86-27-68755363
[b] Changchun Institute of Applied Chemistry, Chinese Academy of Sciences, Changchun 130022, China. E-mail: mdg1014@ciac.ac.cn
[c] Institute of Chemistry, Chinese Academy of Sciences, Beijing, China

† Electronic supplementary information (ESI) available: TGA, DSC, UV and PL spectra, and detailed devices performances. See DOI: 10.1039/c5tc01028d

‡ The authors contributed equally to this paper.

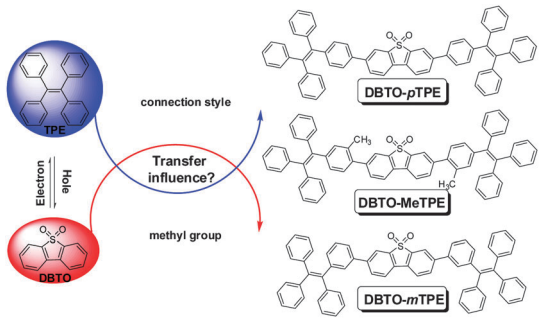

Chart 1 Chemical structures of the three AIEgens.

these three AIEgens exhibit very different transporting properties: **DBTO-*p*TPE** displays good electron-transporting property, while the introduction of methyl groups in **DBTO-MeTPE** induces a better hole-transporting property. More interestingly, **DBTO-*m*TPE** adopted the *meta*-linkage mode, which can bring about ambipolar transporting ability. Herein, we present the synthesis, thermal, photophysical, electrochemical and electroluminescent (EL) properties of these three AIEgens in detail.

Results and discussion

Synthesis

All the three luminogens were easily obtained through a one step palladium(0)-catalyzed Suzuki cross-coupling reaction, with high yields (Scheme 1). All new compounds were purified by column chromatography on a silica gel using petroleum ether–chloroform as the eluent and they were fully characterized using ^{1}H and ^{13}C NMR spectroscopy, mass spectrometry, and elemental analysis.

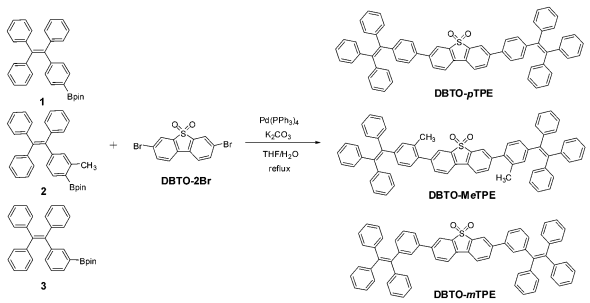

Scheme 1 Synthetic routes to the three AIEgens.

Thermal properties

In general, good thermal stability is beneficial for the process of vacuum deposition and operating stability of OLED devices. The thermal properties of these new compounds were investigated using thermogravimetric analysis (TGA) and differential scanning calorimetry (DSC) measurements.

Because of their rigid structures, these compounds show good thermal stability, with T_d (corresponding to 5% weight loss) values in the range of 426–462 °C (Table 1 and Fig. S1, ESI†). In general, compounds with the *para*-linkage mode show better thermal stability than the ones with *meta*-linkage mode, which is due to their more rigid conformations.[16] Among them, **DBTO-*p*TPE** (462 °C) possesses higher decomposition temperatures than the others. **DBTO-MeTPE** showed a lower T_d of 432 °C, due to the introduction of methyl groups. The glass transition temperatures (T_g) for **DBTO-*p*TPE**, **DBTO-MeTPE** and **DBTO-*m*TPE** are 139, 129 and 110 °C, respectively. Thus, these good thermal properties would be beneficial for the good performance of their corresponding OLED devices.

Photophysical and AIE properties

These compounds have good solubility in common organic solvents such as dichloromethane, chloroform and tetrahydrofuran (THF). In THF, **DBTO-*p*TPE**, **DBTO-MeTPE** and **DBTO-*m*TPE** show absorption maxima at 370, 346 and 302 nm, respectively (Fig. 1), which indicate that compounds with the *para*-linkage mode are more conjugated and that the *meta*-linkage mode can induce poor conjugation. In the UV spectra of their thin films (Fig. S3, ESI†), the λ_{max}s of these compounds are red shifted. However, due to the fact that they have more twisted structures, **DBTO-MeTPE** and **DBTO-*m*TPE** only show small shifts of about 2 nm. This further confirmed that intramolecular conjugation can be inhibited effectively through the introduction of methyl groups and the *meta*-linkage mode.[16]

In view of the introduction of TPE, to investigate the possible AIE characteristics of these luminogens, their fluorescent behaviors were studied. Considering that good and poor solvents should be well miscible, tetrahydrofuran and water were chosen as the solvent pair. Fig. 2 demonstrates the PL change and fluorescent image of **DBTO-*m*TPE** in THF and THF–water mixtures. It can be seen that in dilute THF solution, the emission intensity is very low, which indicates that it is nearly nonemissive in the solution state. However, when a large amount of water is added, intense emission can be observed.

Table 1 The thermal, electrochemical and photophysical data of the luminogens

						PL λ_{em}		Φ_F (%)	$\lambda_{max,abs}$	
	T_d[a] (°C)	T_g[b] (°C)	E_g[c] (eV)	E_{HOMO}[d] (eV)	E_{LUMO}[e] (eV)	Aggr[f] (nm)	Film[g] (nm)	Solv[f]	Solv[h] (nm)	Film[g] (nm)
DBTO-*p*TPE	462	139	2.93	−5.61	−2.68	485	483	34.7(68.3)	370	383
DBTO-MeTPE	432	130	3.10	−5.60	−2.50	475	479	27.5(59.2)	346	355
DBTO-*m*TPE	426	110	3.25	−5.63	−2.38	473	475	27.4(32.8)	320	322

[a] 5% weight loss temperature measured by TGA under N_2. [b] Glass-transition temperature measured by DSC under N_2. [c] Band gap estimated from optical absorption band edge of the solution. [d] Calculated from the onset oxidation potentials of the compounds. [e] Estimated using the empirical equation $E_{LUMO} = E_{HOMO} + E_g$. [f] Determined in THF–water mixtures (f_w = 90%) and in parenthesis is the absolute quantum yield of solid. [g] On glass. [h] Observed from absorption spectra in dilute THF solution, 10 μM.

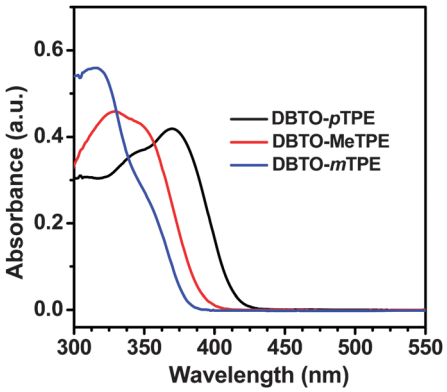

Fig. 1 UV-vis spectra in THF solution (10 μM).

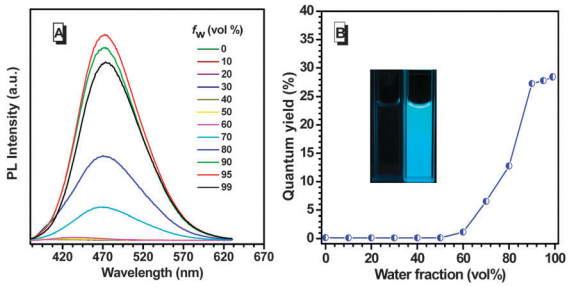

Fig. 2 (A) PL spectra of **DBTO-*m*TPE** in THF–H_2O mixtures with different water fractions (f_w). (B) Plots of fluorescence quantum yields determined in THF–H_2O solutions using 9,10-diphenylanthracene (Φ = 90% in cyclohexane) as the standard *versus* water fractions. Inset in (B): images of **DBTO-*m*TPE** in THF–water mixtures (f_w = 0 and 99%) taken under the illumination of a 365 nm UV lamp.

When the water fraction is over 50%, the PL intensity increases swiftly due to the formation of aggregates. At an f_w value of 99%, the PL intensity is the highest, with a peak located at 483 nm for **DBTO-*m*TPE**, which is about 150-fold higher than that in pure THF. Similar phenomena were also observed for **DBTO-*p*TPE** and **DBTO-MeTPE** (Fig. S5 and S6, ESI†). The quantitative enhancement of emission was evaluated by PL quantum yields (Φ_F) using 9,10-diphenylanthracene as the standard. From a pure solution in THF to aggregate states in 99% aqueous mixtures, the Φ_F value of **DBTO-*p*TPE** increased from 0.21% to 34.43%. This value increases from 0.086% and 0.15% to 29.04% and 28.44% for **DBTO-MeTPE** and **DBTO-*m*TPE**, respectively. When the water fraction was less than 50%, the Φ_F values were all in the range of 0.1–0.4%, which indicate that all the three luminogens are AIE-active.

Electrochemical properties and theoretical calculations

Cyclic voltammetry (CV) measurements (Fig. 3) were carried out to investigate the electrochemical properties of the new AIEgens. Their highest occupied molecular orbital (HOMO) energy levels were estimated from their onset oxidation potentials according to the equation: HOMO = $-(4.8 + E_{ox})$ eV, while their lowest unoccupied molecular orbital (LUMO) energy levels were obtained from their optical band-gap energies (estimated from

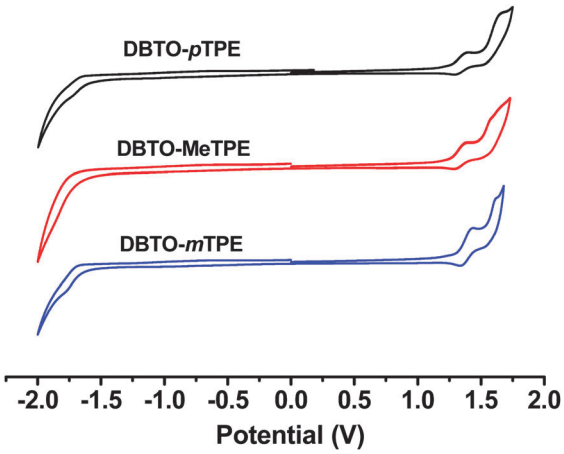

Fig. 3 Cyclic voltammograms recorded in dichloromethane.

the onset wavelengths of their UV absorptions) and HOMO values. For **DBTO-*p*TPE**, **DBTO-MeTPE** and **DBTO-*m*TPE**, their HOMO values were calculated to be −5.61, −5.60 and −5.63 eV, while their corresponding LUMO energy levels were −2.68, −2.50 and −2.38 eV, respectively. Through different linkage modes and the introduction of methyl groups, the HOMO values are almost unchanged, but the LUMO energy levels showed some differences. The LUMO energy level of **DBTO-*p*TPE** is very close to the LUMO value of TPBi; thus, a good transfer of electrons can be expected.

To obtain some information at the molecular level, density functional theory (DFT) calculations (B3LYP/6-31g*) were carried out in order to obtain the optimized structures and orbital distributions of the HOMO and LUMO energy levels. As demonstrated in Fig. 4, the electron clouds of the HOMO energy levels are all mainly located at the periphery TPE units, while the LUMOs are dominated by orbitals from dibenzothiophene *S*,*S*-dioxide. It can be found that the electron clouds are more delocalized in the HOMO of **DBTO-*p*TPE**, while for **DBTO-*m*TPE**, the electron clouds of the HOMO energy level are just located at the TPE. This may be caused by the difference in conjugation between the DBTO and TPE units. The predicted values of the band-gaps for **DBTO-*p*TPE**, **DBTO-MeTPE** and **DBTO-*m*TPE** were calculated to be 3.35, 3.46, 3.52 eV, respectively, which are about 0.4 eV larger than their optical band-gaps. From the optimized structures, the angles between the DBTO unit and the adjacent benzene are found to be 35.4°, 50.8° and 37.6°. The twist degree of the three AIEgens is as follows: **DBTO-*p*TPE** < **DBTO-*m*TPE** < **DBTO-MeTPE**.

Single-carrier devices

To verify whether our strategy of different linkage modes and adjustment of the conjugation effect can affect the transport properties of the AIEgens, hole- and electron-only devices were fabricated with the respective configurations of ITO/MoO_3 (8 nm)/X (15 nm)/MoO_3 (8 nm)/Al and ITO/LiF (1 nm)/X (15 nm)/LiF (1 nm)/Al. In these devices, MoO_3 worked as the hole-injection and electron-blocking layers, LiF as the electron-

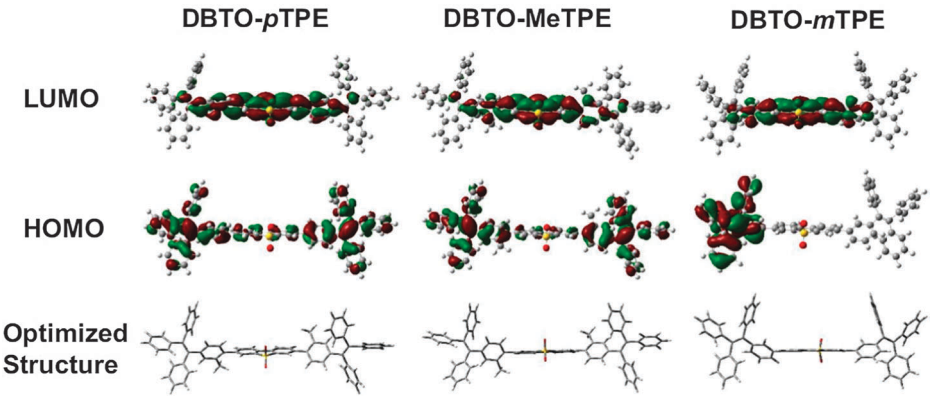

Fig. 4 Calculated molecular orbital amplitude plots of HOMO and LUMO levels and optimized molecular structures.

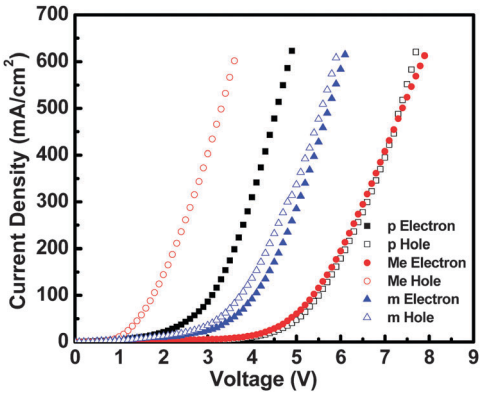

Fig. 5 Current density–voltage characteristics of hole- and electron-only devices of **DBTO-*p*TPE** (*p*), **DBTO-MeTPE** (Me) and **DBTO-*m*TPE** (*m*).

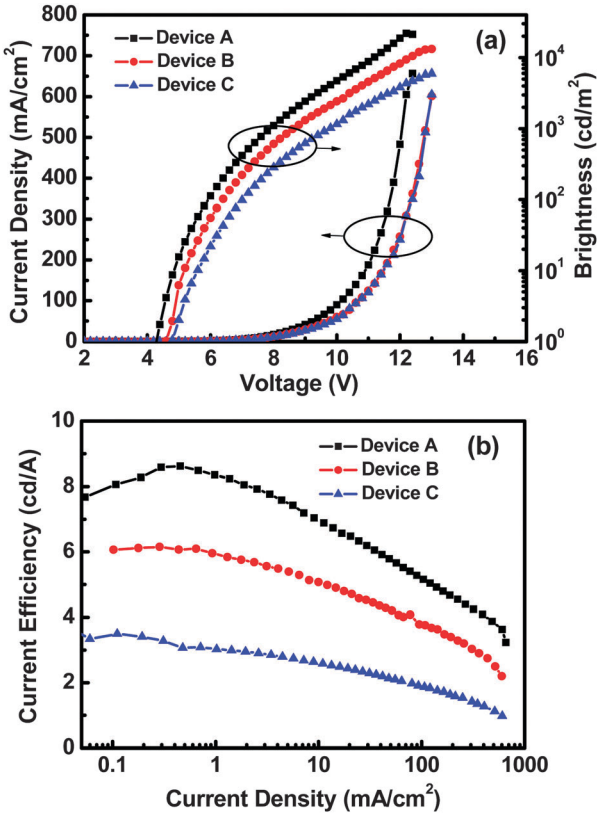

Fig. 6 (a) Current density–voltage-luminance characteristics and (b) change in current efficiency with the current density in multilayer EL devices of the AIEgens **DBTO-*p*TPE** (device A), **DBTO-MeTPE** (device B) and **DBTO-*m*TPE** (device C).

injection layers and X refers to **DBTO-*p*TPE**, **DBTO-MeTPE** or **DBTO-*m*TPE**. Fig. 5 shows their current density–voltage (*J*–*V*) characteristics, and different transport properties can be seen. Among them, the device based on **DBTO-*p*TPE** displays good electron-transporting property, while the transfer ability of holes is relatively weak, which indicates that the major carriers are electrons. In contrast, the introduction of methyl groups could induce a better hole-transporting property, considering that both **DBTO-*p*TPE** and **DBTO-MeTPE** adopted the same linkage mode and the introduction of methyl could induced larger twist angle (50.8°) between TPE and DBTO units. The totally different transport properties were caused by the conjugation and the interaction that followed between the TPE and DBTO units. More interestingly, **DBTO-*m*TPE** adopted a *meta*-linkage mode, which can bring about balanced hole- and electron-transporting ability, namely, the ambipolar transporting ability. This is possibly due to its poor conjugation when the *meta*-linkage mode is adopted. This is beneficial to keep the respective carrier transport, even though there are other influencing factors such as the stacking behavior and dipole interaction. In this system, different linkage modes and adjustment of the conjugation effect can indeed influence the transport properties, thus providing valuable guidance for the further design of AIEgens.

The results also confirm that in order to yield AIEgens with balanced hole and electron mobility, there should be some interactions between the p- and n-type groups, but the interaction should be very weak. This is almost the same for the design of excellent host materials for phosphorescent luminogens with good ambipolar transporting ability. Thus, the present strategies for the design of good host materials might be directly applied to the further development of AIEgens with balanced hole and electron mobility. In addition, perhaps, the reported excellent

host materials might be offered AIE characteristics to yield good AIEgens with ambipolar transporting capacity. As the AIE research field is very promising, our findings might stimulate some new applications of AIEgens that are related to their transporting properties.

Characterization of fluorescent OLEDs

Their good thermal property and efficient solid-state emission also encouraged us to investigate the EL performance of the three AIEgens. Nondoped fluorescent OLEDs were fabricated with the configuration of ITO/MoO_3 (10 nm)/NPB (60 nm)/mCP (10 nm)/EML (15 nm)/TPBi (30 nm)/LiF (1.5 nm)/Al (100 nm). In these OLED devices, 1,4-bis(1-naphthylphenylamino)-biphenyl (NPB), 1,3-di(9H-carbazol-9-yl)benzene (mCP) and 1,3,5-tris(*N*-phenylbenzimidazol-2-yl)benzene (TPBi) were used as hole-transporting, electron-blocking and electron-transporting layers, respectively. Fig. S9 (ESI†) shows the EL spectra of these devices at different driving voltages. Their EL spectra are almost identical to the corresponding PL spectra of their solid thin films, and show little change under different driving voltages. These spectral characteristics imply a good confinement of excitons in the emission layers,[23,24] which is derived from the large band gaps of the adjacent mCP (3.5 eV) and TPBI (3.5 eV) layers. The performances of these devices are shown in Fig. 6 and Table 2. Devices based on **DBTO-*p*TPE** turn on at a lower voltage of 4.3 eV in comparison with the devices based on **DBTO-MeTPE** (4.6 eV) or **DBTO-*m*TPE** (4.8 eV), which indicate smaller injection barriers between the transporting layers and emitters. From the energy diagram (Fig. S11, ESI†), the HOMO levels are almost identical, but the LUMO level of **DBTO-*p*TPE** is closer to that of TPBi, hence the transfer of electrons play an important role as mentioned above.[25] Among the devices fabricated, the device based on **DBTO-*p*TPE** exhibits the highest efficiencies with the maximum external quantum efficiency ($\eta_{ext,max}$) of 3.62%, current efficiency ($\eta_{C,max}$) of 8.66 cd A^{-1}, and power efficiency ($\eta_{P,max}$) of 5.28 lm W^{-1}. For **DBTO-MeTPE** and **DBTO-*m*TPE**, their λ_{max}s are centered at 481 and 480 nm, respectively, and are blue shifted to a shorter wavelength compared to that of **DBTO-*p*TPE** (488 nm), which fits our expectation as previously reported.[15,16] The blue emission devices exhibited CE of 6.17 and 3.51 cd A^{-1} for **DBTO-MeTPE** and **DBTO-*m*TPE**, respectively, which further show that the introduction of methyl groups is more efficient to achieve highly efficient blue emission than the *meta*-linkage mode. For **DBTO-*m*TPE**, its ambipolar property did not induce the highest efficiency, which further implies that device performance can be affected by various factors such as device structure, charge injection, and exciton block.[26–28]

Table 2 Detailed EL performances of devices based on **DBTO-*p*TPE** (A), **DBTO-MeTPE** (B) and **DBTO-*m*TPE** (C)[a]

Device	V_{on} (V)	L_{max} (cd m^{-2})	$\eta_{p,max}$ (lm W^{-1})	$\eta_{c,max}$ (cd A^{-1})	$\eta_{ext,max}$ (%)	CIE (x, y)
A	4.3	21 984	5.28	8.66	3.62	0.19, 0.36
B	4.6	13 218	3.82	6.17	3.01	0.17, 0.28
C	4.8	5957	2.11	3.51	1.81	0.17, 0.26

[a] Abbreviations: V_{on} = turn-on voltage at 1 cd m^{-2}, L_{max} = maximum luminance, $\eta_{p,max}$, $\eta_{c,max}$ and $\eta_{ext,max}$ = maximum power, current and external efficiencies, respectively. CIE = Commission International de l'Éclairage coordinates at 8 V.

Conclusions

In conclusion, through different linkage modes and the adjustment of conjugation, three AIEgens were constructed using tetraphenylethene and dibenzothiophene-*S*,*S*-dioxide. All the luminogens exhibited typical aggregation induced emission. More importantly, different transport properties can be realized simply through different linkage modes and the adjustment of conjugation. **DBTO-*p*TPE** displayed good electron-transporting property, while **DBTO-MeTPE** and **DBTO-*m*TPE** showed hole-transporting property and ambipolar transporting ability. When used in multilayer OLEDs, **DBTO-*p*TPE** exhibited the highest efficiencies with the maximum external quantum efficiency of 3.62% and current efficiency of 8.66 cd A^{-1}. The blue emission devices exhibited the current efficiencies of 6.17 and 3.51 cd A^{-1} for **DBTO-MeTPE** and **DBTO-*m*TPE**, respectively. Thus, taking their transport properties into account, the obtained experimental results might open up a new option for the design of efficient blue AIEgens.

Experimental section

Characterization

THF was dried over and distilled from K–Na alloy under an argon atmosphere. All other chemicals and reagents were purchased from commercial suppliers and were used without further purification unless otherwise specified.

^{1}H and ^{13}C NMR spectra were obtained on a MECUYRVX300 spectrometer. Elemental analyses of carbon, hydrogen, and nitrogen were performed on a CARLOERBA-1106 micro analyzer. Mass spectra were obtained on a ZAB 3F-HF spectrometer. MS (EI) were recorded on a Finnigan PRACE mass spectrometer. UV-vis absorption spectra were obtained on a Shimadzu UV-2500 recording spectrometer. Photoluminescence spectra were obtained on a Hitachi F-4500 fluorescence spectrometer. Differential scanning calorimetry (DSC) was performed on a Mettler Toledo DSC 822e at a heating and cooling rate of 10 °C min^{-1} from room temperature to 200 °C under nitrogen. The glass transition temperature (T_g) was determined from the first heating scan, except if otherwise stated. Thermogravimetric analysis (TGA) was undertaken with a NETZSCH STA 449C instrument. The thermal stability of the samples under a nitrogen atmosphere was determined by measuring their weight loss while heating at a rate of 10 °C min^{-1} from 25 to 600 °C. Cyclic voltammetry (CV) was carried out on a CHI voltammetric analyzer in a three-electrode cell with a Pt counter electrode, an Ag/AgCl reference electrode, and a glassy carbon working electrode at a scan rate of 100 mV s^{-1} with 0.1 M tetrabutylammonium perchlorate (purchased from Alfa Aesar) as the supporting electrolyte, in anhydrous dichloromethane

solution purged with nitrogen. The potential values that were obtained with reference to the Ag/Ag^+ electrode were converted to values *versus* the saturated calomel electrode (SCE) by means of an internal ferrocenium/ferrocene (Fc^+/Fc) standard.

Computational details

The geometrical and electronic properties were optimized at the B3LYP/6-31g(d) level using the Gaussian 09 program. The molecular orbitals were obtained at the same level of theory.

Device fabrication and measurement

The hole-transporting material, NPB (1,4-bis(1-naphthylphenylamino)-biphenyl), and electron-transporting material, 1,3,5-tris(*N*-phenylbenzimidazol-2-yl)benzene (TPBi), were obtained from a commercial source. The EL devices were fabricated by vacuum deposition of the materials at a base pressure of 10^{-6} Torr onto a glass that was precoated with a layer of indium tin oxide (ITO) with a sheet resistance of 25 Ω per square. Before the deposition of an organic layer, the clear ITO substrates were treated with oxygen plasma for 2 min. The deposition rate of organic compounds was 1–2 Å s^{-1}. Finally, a cathode composed of lithium fluoride (1 nm) and aluminium (100 nm) was sequentially deposited onto the substrate under the vacuum of 10^{-6} Torr. The *L–V–J* of the devices was measured with a Keithey 2400 Source meter and a Keithey 2000 Source multimeter equipped with a calibrated silicon photodiode. The EL spectra were obtained using a JY SPEX CCD3000 spectrometer. Absolute PL quantum yields of the powders were measured on a HAMAMATSU C11347 spectrometer. All measurements were carried out at room temperature under ambient conditions.

Preparation of compounds

3,7-Dibromo-dibenzothiophene-*S*,*S*-dioxide and the boronic acid esters **1**, **2** and **3** were all synthesized according to literature procedures.[16,18] All other chemicals and reagents were obtained from commercial sources and were used as received without further purification. Solvents for chemical synthesis were purified according to standard procedures.

Synthesis of DBTO-*p*TPE

A mixture of compound 1 (306 mg, 0.67 mmol), 3,7-dibromo-dibenzothiophene-*S*,*S*-dioxide (100 mg, 0.27 mmol), $Pd(PPh_3)_4$ (30 mg) and potassium carbonate (740 mg, 5.36 mmol) in THF (10 mL) and distilled water (2.7 mL) was refluxed for 24 h under nitrogen in a 100 mL Schlenk tube. The mixture was extracted with dichloromethane. The combined organic extracts were dried over anhydrous Na_2SO_4 and concentrated by rotary evaporation. The crude product was purified by column chromatography on a silica gel using dichloromethane/petroleum ether as the eluent to afford the product as a green powder in the yield of 87% (206 mg). ^{1}H NMR (300 MHz, $CDCl_3$) δ (ppm): 7.98 (s, 2H), 7.81 (s, 4H), 7.39 (d, J = 8.1 Hz, 4H), 7.06–7.13 (m, 34H). ^{13}C NMR (75 MHz, $CDCl_3$) δ (ppm): 144.2, 143.4, 143.3, 143.1, 141.7, 140.0, 138.5, 13 6.4, 132.1, 131.3, 129.9, 127.8, 127.6, 126.7, 126.6, 126.5, 126.1, 121.7, 120.4. MS (EI), *m*/*z*: 876.18 ([M^+], calcd for $C_{64}H_{44}O_2S$, 876.31). Anal. calcd for $C_{64}H_{44}O_2S$: C, 87.64; H, 5.06; S, 3.66. Found: C, 87.39; H, 5.22; S, 3.64.

Synthesis of DBTO-MeTPE

A mixture of compound **2** (483 mg, 1.02 mmol), 3,7-dibromo-dibenzothiophene-*S*,*S*-dioxide (152 mg, 0.41 mmol), $Pd(PPh_3)_4$ (40 mg) and potassium carbonate (1.13 g, 8.20 mmol) in THF (15 mL) and distilled water (4.1 mL) was refluxed for 24 h under nitrogen in a 100 mL Schlenk tube. The mixture was extracted with dichloromethane. The combined organic extracts were dried over anhydrous Na_2SO_4 and concentrated by rotary evaporation. The crude product was purified by column chromatography on silica gel using dichloromethane/petroleum ether as the eluent to afford the product as a light green powder in the yield of 75% (278 mg). ^{1}H NMR (300 MHz, $CDCl_3$) δ (ppm): 7.82 (d, J = 8.4 Hz, 2H), 7.75 (s, 2H), 7.59 (d, J = 7.8 Hz, 2H), 7.10–7.14 (m, 30H), 6.91–7.00 (m, 6H), 2.11 (s, 6H). ^{13}C NMR (75 MHz, $CDCl_3$) δ (ppm): 144.2, 143.7, 143.5, 143.4, 141.4, 140.2, 137.8, 137.4, 134.8, 134.2, 133.6, 131.3, 131.2, 129.8, 129.2, 128.8, 127.7, 127.6, 126.6, 126.5, 126.4, 122.8, 121.1, 20.3. MS (EI), *m*/*z*: 904.34 ([M^+], calcd for $C_{66}H_{48}O_2S$, 904.34). Anal. calcd for $C_{66}H_{48}O_2S$: C, 87.58; H, 5.35; S, 3.54. Found: C, 87.34; H, 5.50; S, 3.53.

Synthesis of DBTO-*m*TPE

A mixture of compound 3 (467 mg, 1.02 mmol), 3,7-dibromo-dibenzothiophene-*S*,*S*-dioxide (152 mg, 0.41 mmol), $Pd(PPh_3)_4$ (40 mg) and potassium carbonate (1.13 g, 8.20 mmol) in THF (15 mL) and distilled water (4.1 mL) was refluxed for 24 h under nitrogen in a 100 mL Schlenk tube. The mixture was extracted with dichloromethane. The combined organic extracts were dried over anhydrous Na_2SO_4 and concentrated by rotary evaporation. The crude product was purified by column chromatography on a silica gel using dichloromethane/petroleum ether as the eluent to afford the product as a white powder in the yield of 82% (294 mg). ^{1}H NMR (300 MHz, $CDCl_3$) δ (ppm): 7.72 (d, J = 8.1 Hz, 2H), 7.52 (s, 2H), 7.47 (d, J = 7.8 Hz, 2H), 7.22–7.24 (m, 8H), 7.05–7.13 (m, 26H). ^{13}C NMR (75 MHz, $CDCl_3$) δ (ppm): 144.3, 143.7, 143.5, 143.3, 143.1, 141.8, 140.2, 138.4, 138.0, 132.3, 131.3, 131.2, 130.6, 129.9, 128.4, 128.0, 127.8, 127.7, 126.9, 126.6, 126.5, 124.9, 121.5, 120.8. MS (EI), *m*/*z*: 876.13 ([M^+], calcd for $C_{64}H_{44}O_2S$, 876.31). Anal. calcd for $C_{64}H_{44}O_2S$: C, 87.64; H, 5.06; S, 3.66. Found: C, 87.71; H, 5.19; S, 3.62.

Acknowledgements

We are grateful to the National Science Foundation of China (no. 21325416, 51333007) and the National Fundamental Key Research Program (2013CB834701, 2013CB834805) for financial support.

Notes and references

1 J. Luo, Z. Xie, J. W. Y. Lam, L. Cheng, H. Chen, C. Qiu, H. S. Kwok, X. Zhan, Y. Liu, D. Zhu and B. Z. Tang, *Chem. Commun.*, 2001, 1740.

2 K. Hatano, H. Saeki, H. Yokota, H. Aizawa, T. Koyama, K. Matsuoka and D. Terunuma, *Tetrahedron Lett.*, 2009, **50**, 5816.
3 Y. Liu, S. Chen, J. W. Y. Lam, P. Lu, R. T. Kwok, F. Mahtab, H. S. Kwok and B. Z. Tang, *Chem. Mater.*, 2011, **23**, 2536.
4 H. Shi, J. Liu, J. Geng, B. Z. Tang and B. Liu, *J. Am. Chem. Soc.*, 2012, **134**, 9569.
5 W. Yuan, P. Lu, S. Chen, J. W. Y. Lam, Z. Wang, Y. Liu, H. S. Kwok, Y. Ma and B. Z. Tang, *Adv. Mater.*, 2010, **22**, 1.
6 J. Y. Kim, T. Yasuda, Y. S. Yang and C. Adachi, *Adv. Mater.*, 2013, **25**, 2666.
7 Z. Zhao, Z. Li, J. W. Y. Lam, J. L. Maldonado, G. Ramos-Ortiz, Y. Liu, W. Yuan, J. Xu, Q. Miao and B. Z. Tang, *Chem. Commun.*, 2011, **47**, 6924.
8 X. Zhang, Y. Zhen, X. Fu, J. Liu, X. Lu, P. He, H. Dong, H. Zhang, G. Zhao, L. Jiang and W. Hu, *J. Mater. Chem. C*, 2014, **2**, 8222.
9 H. Chen, W. Y. Lam, J. Luo, Y. L. Ho, B. Z. Tang, D. Zhu, M. Wong and H. S. Kwok, *Appl. Phys. Lett.*, 2002, **81**, 574.
10 W. Chen, Y. Yuan, G. Wu, H. Wei, J. Ye, M. Chen, F. Lu, Q. Tong, F. Wong and C. S. Lee, *Org. Electron.*, 2015, **17**, 159.
11 Y. Tao, C. Yang and J. Qin, *Chem. Soc. Rev.*, 2011, **40**, 2943.
12 W. Yuan, P. Lu, S. Chen, J. W. Y. Lam, Z. Wang, Y. Liu, H. S. Kwok, Y. Ma and B. Z. Tang, *Adv. Mater.*, 2010, **22**, 1.
13 W. Yuan, Y. Gong, S. Chen, X. Shen, J. W. Y. Lam, P. Lu, Y. Lu, Z. Wang, R. Hu, N. Xie, H. S. Kwok, Y. Zhang, J. Sun and B. Z. Tang, *Chem. Mater.*, 2012, **24**, 1518.
14 Y. Liu, X. Tao, F. Wang, X. Dang, D. zou, Y. Ren and M. Jiang, *J. Phys. Chem. C*, 2008, **112**, 3975.
15 J. Huang, N. Sun, Y. Dong, R. Tang, P. Lu, P. Cai, Q. Li, D. Ma, J. Qin and Z. Li, *Adv. Funct. Mater.*, 2013, **23**, 2329.
16 J. Huang, N. Sun, J. Yang, R. Tang, Q. Li, D. Ma and Z. Li, *Adv. Funct. Mater.*, 2014, **24**, 7645.
17 J. Huang, N. Sun, P. Cheng, R. Tang, Q. Li, D. Ma and Z. Li, *Chem. Commun.*, 2014, **50**, 2136.
18 I. I. Perepichka, I. F. Perepichka, M. R. Bryce and L. O. Pålsson, *Chem. Commun.*, 2005, 3397.
19 T. H. Huang, J. T. Lin, L. Y. Chen, Y. T. Lin and C. C. Wu, *Adv. Mater.*, 2006, **18**, 602.
20 R. He, S. Hu, J. Liu, L. Yu, B. Zhang, N. Li, W. Yang, H. Wu and J. Peng, *J. Mater. Chem.*, 2012, **22**, 3440.
21 L. Yu, J. Liu, S. Hu, W. Yang, H. Wu, J. Peng, R. Xia and D. D. C. Bradley, *Adv. Funct. Mater.*, 2013, **23**, 4366.
22 Y. Yang, L. Yu, Y. Xue, Q. Zou, B. Zhang, L. Ying, W. Yang, J. Peng and Y. Cao, *Polymer*, 2014, **55**, 1698.
23 J. Ye, Z. Chen, M. K. Fung, C. Zeng, X. Ou, X. Zhang, Y. Yuan and C. S. Lee, *Chem. Mater.*, 2013, **25**, 2630.
24 S. Y. Lee, T. Yasuda, Y. S. Yang, Q. Zhang and C. Adachi, *Angew. Chem., Int. Ed.*, 2014, **53**, 6402.
25 Y. Yuan, J. Chen, F. Lu, Q. Tong, Q. Yang, H. W. Mo, T. W. Ng, F. L. Wong, Z. Guo, J. Ye, Z. Chen, X. Zhang and C. S. Lee, *Chem. Mater.*, 2013, **25**, 4957.
26 X. Zhan, N. Sun, Z. Wu, J. Tu, L. Yuan, X. Tang, Y. Xie, Q. Peng, Y. Dong, Q. Li, D. Ma and Z. Li, *Chem. Mater.*, 2015, **27**, 1847.
27 M. Zhu and C. Yang, *Chem. Soc. Rev.*, 2013, **42**, 4963.
28 G. M. Farinola and R. Ragni, *Chem. Soc. Rev.*, 2011, **40**, 3467.